eprints@whiterose.ac.uk
https://eprints.whiterose.ac.uk/

On the Analysis of Cellular Networks with Caching and Coordinated Device-to-Device Communication

Asma Afzal[†], Syed Ali Raza Zaidi[†], Des McLernon[†] and Mounir Ghogho[†‡]

[†]School of Electronic and Electrical Engineering, University of Leeds, United Kingdom
[‡]International University of Rabat, Morocco
Email: {elaaf, s.a.zaidi, d.c.mclernon, m.ghogho}@leeds.ac.uk

Abstract—In this paper, we develop a comprehensive analytical framework for cellular networks that are enhanced with coordinated device-to-device (D2D) communication, where the D2D devices are equipped with content caching capabilities. The base station (BS) coordinates the D2D communication by establishing a D2D link between the requesting user and the nearest D2D helper within the same cell if the latter contains the requested content, otherwise, the BS serves the user itself. The motivation behind restricting D2D pairs within a macro cell is to make coordinated D2D communication realizable as the BS can keep track of the content of the devices without the increased overhead of inter-BS coordination. This approach is similar to LTE direct, where D2D pairing is managed by the BS. We model the locations of BS and D2D helpers using a homogeneous Poisson point process (HPPP). The distribution of the distance between the tagged user and its neighboring D2D helper within the cell is derived using disk approximation for the Voronoi cell, which is shown to be reasonably accurate. We fully characterize the cellular and D2D coverage and the link spectral efficiency of such a network. Our results reveal that cache enabled D2D communication becomes more effective as the requesting user moves away from the BS and high performance gains can be achieved compared to conventional cellular networks, especially when the popularity distribution is skewed and most popular files are requested.

I. INTRODUCTION

Ubiquitous devices such as smart phones and tablets have fueled the demand for data intensive applications including live video streaming, social networking and e-gaming. Recent observations have indicated that the downloaded multimedia content consists of a lot of duplications of a few very popular files [1]. As a consequence, current research on fifth generation (5G) wireless networks is geared towards developing intelligent ways of data dissemination by deviating from the traditional host centric network architecture to a more versatile information centric architecture. Direct device-to-device (D2D) communication is seen as a promising candidate to serve this purpose [2]. Mobile users in close physical proximity can exchange popular files without the intervention of the base station (BS). This not only offloads the burden of duplicate transmissions from the BS, but it also provides higher rates due to short range D2D communication [3].

Several techniques have been proposed to materialize the concept of integration of D2D communication with cellular networks. Major design questions are: Should D2D communication operate in the licensed spectrum or unlicensed spectrum,

and in the licensed spectrum should it be underlay or overlay, coordinated by the BS or uncoordinated. The reader is referred to a detailed discussion of these design questions in [4] and the references therein. In this paper, we focus on coordinated overlay D2D communication, where a macro base station (MBS) establishes, manages and arbitrates a D2D connection [5]. The MBS schedules the transmission between the requesting user and its neighboring device if the latter possesses the requested content, otherwise, the BS serves the requesting user from its own cache or by retrieving it from the content provider through the core network. Our goal is to borrow tools from stochastic geometry to quantify the improvement in D2D performance in this scenario. Stochastic geometry has recently emerged as a powerful tool to develop tractable framework to analyze the performance of large scale cellular networks [6]. A broad range of the available literature on the analysis of overlaid D2D communication using stochastic geometry focuses on various performance metrics including spectrum allocation and mode selection [7]–[9]. The authors, however, do not take content popularity and storage into consideration. In [10], a clustered D2D network with caching and a Zipf type content popularity distribution is considered. The hypothetical clustering ensures a finite number of D2D links inside the cluster and the D2D network operates in isolation from the cellular network, i.e outage occurs if neighboring devices do not have the requested content. We take a step forward towards a more realistic scenario to analyze a network where a requesting user is served by the MBS if D2D communication is infeasible.

The main contributions of this article are summarized as follows. We assume that both the MBSs and D2D helpers are distributed according to independent homogeneous Poisson point processes (HPPPs). We derive the distribution of the distance between the requesting user and the nearest D2D helper within the cell using disk approximation with a variable radius ρ_{mid} (described later in Section III). With the help of this approximation, we obtain useful insights into the worst case performance when the requesting user is at the cell edge. We also characterize the cellular and D2D coverage probabilities and the link spectral efficiency (LSE) for the requesting user. The distance between the MBS and its tagged requesting user, d, enables us to gauge the effectiveness of the coordinated D2D communication. We show that as the

separation between the tagged user and the MBS increases, cellular communication becomes more and more unreliable while D2D communication is not as badly affected. We show that the coordinated D2D communication results in significant performance gains in terms of LSE especially when the file popularity distribution is skewed and popular contents are requested.

The remainder of this paper is organized as follows: Section II describes the spatial setup, signal propagation, content popularity and caching models. Section III provides the derivation of the distance between the tagged user and the nearest D2D helper within the cell. The distribution of this distance is then used to characterize the LSE in Section IV. Section V discusses the results compares our analysis with network simulations. Section VI concludes the paper.

II. SYSTEM MODEL

We consider a cellular downlink (DL) scenario of MBSs which are overlaid with D2D helpers. These D2D helper devices can be considered as users which are not receiving any data form the MBS in the current resource block and can transmit their data. The MBS schedules a user with its neighboring D2D helper inside the cell if the helper has the requested file. The discussion on the modeling details and the key assumptions now follow.

A. Spatial Model and User Association

We consider that both the MBS and D2D helpers are distributed according to the independent HPPPs Φ_M and Φ_D with intensities λ_M and λ_D respectively, where $\lambda_D \gg \lambda_M$. Each user associates with the nearest MBS. The association region is defined as

$$\mathcal{S}_i \overset{def}{=} \left\{ \mathbf{x} \in \mathbb{R}^2 \, : \, \|\mathbf{y}_i - \mathbf{x}\| < \|\mathbf{y}_j - \mathbf{x}\|, \forall \mathbf{y}_j \in \Phi_M, j \neq i \right\}, \quad (1)$$

where $\mathcal{S}_i$ represents a Voronoi cell of the MBS $\mathbf{y}_i \in \Phi_M$. The performance is measured at the tagged requesting user at the location $\mathbf{x}_t$ at a distance d from the typical MBS[1] ($\|\mathbf{x}_t\| = d$, see Fig. 1). The tagged user may also be served by the neighboring D2D helper $\mathbf{z}_i$ within the typical cell depending on the content availability, where $\{\mathbf{z}_i \, : \, \|\mathbf{z}_i - \mathbf{x}_t\| < \|\mathbf{z}_j - \mathbf{x}_t\|, \mathbf{z}_j \in \Phi_D \cap \mathcal{S}_0, \mathbf{x}_t \in \mathcal{S}_0, j \neq i.\}$ Fig. 1 shows a realization of this spatial setup. It is important to mention that in our analysis, we condition the network such that the tagged user at the distance d always lies inside the typical cell. This is to ensure that the tagged user associates with the typical BS ($y_i = y_0$ and $\mathcal{S}_i = \mathcal{S}_0$ in (1)). We further assume that there is at least one D2D helper for the tagged user inside the typical cell not necessarily with the desired data. The MBS examines whether the content is present in the neighboring D2D helper's cache before serving the user.

---

[1]Without any loss of generality, we assume that the MBS is located at the origin. This follows from the palm distribution of HPPPs and Slivnyak's theorem [11].
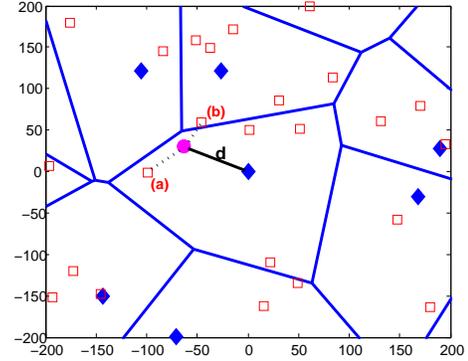

Figure 1: Spatial model of the network. MBSs are depicted by blue, filled diamonds; D2D helpers by red squares; and requesting user by a filled magenta circle. Note that the nearest same cell D2D helper for the requesting user is (a), although (b) is actually closer, but in a different cell.

B. Propagation Model and Spectrum Access

We assume that both the cellular and D2D links experience channel impairments including path loss and small-scale Rayleigh fading. The power received at $\mathbf{x}_t$ from the MBS/ D2D helper located at $\mathbf{y} \in \Phi_K, K = \{M, D\}$ is given as,

$$P_r = P_K h(\mathbf{y}, \mathbf{x}_t) \|\mathbf{y} - \mathbf{x}\|^{-\alpha} \text{ Watts}, \quad (2)$$

where P_M and P_D are the transmit powers of the macro BS and D2D helper respectively, α represents the path loss exponent ranging between 2 and 5 and $h(\mathbf{a}, \mathbf{b})$ is the channel power for the link $\mathbf{a}$ to $\mathbf{b}$. We assume that $h(\mathbf{a}, \mathbf{b})$ is an i.i.d unit-mean exponential RV representing the squared-envelope of Rayleigh fading and hence we will simply denote the channel gain by h for conciseness. We consider an in-band overlay spectrum access strategy restricting our analysis to the performance over a single channel. We assume that there is universal frequency reuse across the network, but the number of resource blocks is greater than the number of users within the cell and hence, there is no intra-cell interference.

C. Content Popularity and Caching Model

The performance of caching is crucially determined by the content popularity distribution. It has been observed that the popularity of data follows a Zipf popularity distribution, where the popularity of the ith file is proportional to the inverse of i^ζ for some real, positive, skewness parameter ζ. It is mathematically represented as

$$pop(i) = \frac{i^{-\zeta}}{\sum_{n=1}^{L} n^{-\zeta}} \quad 1 \leq i \leq L. \quad (3)$$

The term in the denominator of (3) is the distribution normalizing factor and L is the file library size. $\zeta = 0$ corresponds to uniform popularity while a higher value of ζ results in a more skewed distribution. Empirical evidence shows that the value for ζ exists from 0.6 to 0.8 for different content types

including web, file sharing, user generated content (UGC) and video on demand (VoD) [12]. We consider that the D2D helper with memory size C_D, stores content i in each memory slot independently according to $pop(i)$. The hit rate for content i, which is the probability that content i is present in a D2D helper's memory, is given as

$$
\begin{aligned}
hit_D(i) &= 1 - \mathbb{P}[i\text{th file not present in } C_D \text{ memory slots}] \\
&= 1 - [1 - pop(i)]^{C_D}. \quad (4)
\end{aligned}
$$

We assume that user requests follow the independent reference model (IRM) as introduced in [12]. The user requests for a file in the library are independently generated following the popularity distribution and there is no spatio-temporal locality, i.e. identical contents have the same popularity in space and time [13]. Furthermore, we assume that all files have a unit size. Our analysis can easily be extended for variable file sizes as each memory slot will then contain a chunk of a file.

III. DISTANCE TO THE NEAREST D2D HELPER WITHIN A MACROCELL

One of the main contributions of this paper is to characterize the distribution of the distance between the tagged user and the nearest D2D helper within the macrocell. It is a well-known fact that the distance between the nearest neighbors for a 2-D Poisson process is Rayleigh distributed and this has been widely adopted for the stochastic geometry analysis of cellular networks [7], [8], [14], [15]. In our case, however, the MBS only keeps a record of the files stored in the memory of D2D helpers within its coverage region. Therefore, it can only connect the requesting user with the helpers within its cell. Fig. 1 illustrates that in our spatial setup, the nearest D2D helper is not always within the macrocell. Hence, this adds a layer of complexity to our model as the distance is no longer independent of the geometrical attributes of the cell, including its shape and size. The distribution of the exact shape and size of a typical Voronoi cell in a 2-D Poisson Voronoi tessellation is still unknown. In their analysis of bivariate Poisson processes in [16], Foss and Zuyev make use of the maximal and minimal disk approximation for the Voronoi cell. The maximal disk, B_{max}, is the largest disk inscribing the Voronoi circle and B_{min} is the smallest circumscribing disk containing the Voronoi cell. The exact characterization of the distribution of the radius ρ_{max} of B_{max} is straight forward as it is the probability that there is no point at a distance $2x$ from the typical MBS and is expressed as $\mathbb{P}[\rho_{max} \geq 2x] = \exp\left(-4\lambda_M \pi x^2\right)$. This implies

$$
f_{\rho_{max}}(x) = 8\lambda_M \pi x \exp(-4\lambda_M \pi x^2), \; x > 0. \quad (5)
$$

There is no exact distribution of ρ_{min}. A few approximations for the CDF exist in literature but they are intractable [17]. We now move away slightly from this notion and introduce a new circular approximation of the Voronoi cell, where the area of the disks is equal to the area of the Voronoi cell. We denote this disk by B_{mid}. We use the subscript *mid* to indicate that the size of this disk lies somewhere in between

the size of B_{min} and B_{max}. The motivation for the same area disk approximation is two fold: 1) according to [18], the Voronoi cells asymptotically converge to circular disks and 2) the average number of D2D helpers inside a cell with this approximation remains the same. In Section V, we show that the selection of the same area approximation for the analysis of distance is fairly accurate. The following Lemma gives the distribuiton of the radius of the approximate disk.

Lemma 1. *The distribution of the radius ρ_{mid} of a disk B_{mid} using same area disk approximation for a Voronoi cell is given as*

$$
f_{\rho_{mid}}(x) = \frac{2(3.5\pi\lambda_M)^{3.5}}{\Gamma(3.5)} x^6 \exp(-3.5\pi\lambda_M x^2) \; x > 0. \quad (6)
$$

Proof: A tight approximation of the distribution of the area of a Voronoi cell from empirical studies is given as [19]

$$
f_A(a) = \frac{(3.5\lambda_M)^{3.5}}{\Gamma(3.5)} a^{2.5} \exp(-3.5\lambda_M \, a). \quad (7)
$$

The same area approximation implies $A = \pi\rho_{mid}^2$. Using the transformation of RVs, we obtain the distribution of $\rho_{mid} = \sqrt{\frac{A}{\pi}}$ in (6). ∎

Based on the above Lemma, we derive the distribution of distance between the tagged user and the nearest D2D helper in the following theorem.

Theorem 1. *The distribution of the distance between the tagged user at the distance d from the MBS and the nearest D2D helper within the typical cell under the same area disk approximation for a Voronoi cell is given as*

$$
\begin{aligned}
f_{R|d}(r) = \frac{1}{p_N(d)} \Bigg[& \int_{\max(d,r-d)}^{r+d} f_1(r,d,x) \, f_{X|X>d}(x) \, dx \\
& + \int_{r+d}^{\infty} f_2(r,d,x) \, f_{X|X>d}(x) \, dx \Bigg], \; X = \{\rho_{max}, \rho_{mid}\} \quad (8)
\end{aligned}
$$

where, $p_N(d) = \int_d^\infty \left[1 - \exp(-\lambda_D \pi x^2)\right] f_{X|X>d}(x) \, dx$, and

$$
f_{R|X}(r) = \begin{cases} f_1(r,d,x) = \lambda_D A_2'(r,d,x) \\ \exp(-\lambda_D A_2(r,d,x)) & x-d < r < x+d, \\ f_2(r,d,x) = 2\pi\lambda_D r \\ \exp(-\lambda_D \pi r^2) & 0 < r < x-d, \end{cases} \quad (9)
$$

where $A_2(r,d,x) = r^2 \arccos\left(\frac{\kappa_1}{2dr}\right) + x^2 \arccos\left(\frac{\kappa_2}{2dx}\right) - \frac{1}{2}\sqrt{4d^2x^2 - \kappa_2^2}$ and $A_2'(r,d,x)$ is the derivative of $A_2(r,d,x)$ with respect to r.

Proof: Please refer to Appendix A ∎

Corollary 1. *The distribution of the distance between the cell-edge user and its nearest D2D helper within the typical cell is given as*

$$f_R(r) = \frac{1}{p_N}\left[\int_{r/2}^{\infty} f_1(r,x)\, f_X(x)\, dx\right],\ X = \{\rho_{max}, \rho_{mid}\},$$

$$(10)$$

where $p_N = \int_0^{\infty} \left[1 - \exp(-\lambda_D \pi x^2)\right] f_X(x)\, dx.$

Proof: For the cell-edge user, $d = x$ and (9) reduces to $f_{R|X=x}(r) = f_1(r,x)\ 0 < r < 2x$. The rest of the proof follows from the proof of Theorem 1. ∎

IV. LINK SPECTRAL EFFICIENCY ANALYSIS

The average LSE for the tagged user requesting the content i can be written as

$$T(i) = hit_D(i)R_D + (1 - hit_D(i))R_M \text{ bps/Hz}, \quad (11)$$

where $hit_D(i)$ is defined in (4) and R_M and R_D are the average normalized cellular and D2D rates respectively. Using a well-known Shannon capacity formulation for the interference limited network, the average normalized rates are expressed as

$$
\begin{aligned}
R_K &= \mathbb{E}\left[\log_2(1 + SIR_K)\right],\ K = \{D, M\} \text{ bps/Hz} \\
&= \frac{1}{\ln(2)}\int_{z>0} (1+z)^{-1}\mathbb{P}\left[SIR_K > z\right] dz, \quad (12)
\end{aligned}
$$

where $K = \{D, M\}$ denotes D2D and cellular link respectively and SIR_K is the signal-to-interference ratio (SIR) in an interference limited scenario, which is given as $SIR_K = h\, l^{-\alpha}/I_K$. Here, $l = \{r, d\}$ is the distance to the nearest D2D helper within the typical cell and the typical MBS respectively, I_K is the inter-cell interference from co-channel transmitters normalized with respect to the transmit power P_K. It is evident from (12) that in order to obtain the average ergodic rates, the distribution of the received SIR needs to be determined. The coverage probability Γ_K is defined as the probability that SIR_K is greater than a certain modulation dependent decoding threshold. It is given as

$$\Gamma_K = \mathbb{P}\left\{\frac{h\, l^{-\alpha}}{I_K} > \tau_K\right\} = \mathbb{E}_l\left[\mathcal{L}_{I_K}(s_K)\right] \quad (13)$$

where $s_K = \tau_K\, l^\alpha$ and $\mathcal{L}_{I_k}(.)$ is the Laplace transform of interference from the active co-channel interferers outside the typical cell. The following theorem gives the coverage probability for the cellular link.

Theorem 2. *The coverage probability of a user at distance d from the MBS being served by the nearest D2D helper within the cell can be expressed as*

$$\Gamma_D \approx \int_{r=0}^{\infty} \exp\left(-2\pi\frac{s_D \tilde{\lambda}_M \delta_D(s_D, \alpha)}{(\alpha - 2)}\right) f_{R|d}(r)\, dr \quad (14)$$

where $\delta_D(s, \alpha) = \mathbb{E}_Q\left[q^{-(\alpha-2)} {}_2F_1\left(1, \beta; 1+\beta; -sq^{-\alpha}\right)\right]$, $\beta = 1 - 2/\alpha$, ${}_2F_1(a,b;c;x)$ *is the generalized hypergeometric function,* $f_Q(q) = 2\pi\tilde{\lambda}_M q \exp(-\tilde{\lambda}_M \pi q^2)$ *and* $\tilde{\lambda}_M = \lambda_M\left[1 - \left(1 + \frac{\lambda_D}{3.5\lambda_M}\right)^{-3.5}\right]$.

Parameter	Value
C_D, L	40, 10^4
ζ, α	0.7, 4
λ_D, λ_M	$200/\pi 500^2$, $20/\pi 500^2$
d	70m

Table I: List of simulation parameters

Proof: Please refer to Appendix B ∎

The following theorem provides the D2D coverage probability of the tagged user.

Theorem 3. *The coverage probability of the tagged user at distance d from the MBS being served by the MBS is given as*

$$\Gamma_M \approx \exp\left(-\lambda_M \delta_M(s_M, \alpha, d)\right) \quad (15)$$

where $\delta_M(s_M, \alpha, d) = \mathbb{E}_\phi\left[\int_{\theta=0}^{2\pi}\int_{v_{min}}^{\infty}\frac{v}{1+s_M^{-1}y^\alpha}dv\, d\theta\right]$, $y = \sqrt{v^2 + d^2 - 2\,d\,v\,\cos(\theta - \phi)}$, *and* $v_{min} = 2d\cos(\theta - \phi)$.

Proof: Please refer to Appendix C. ∎

For the special case of quantifying coverage at the cell edge user, we replace $f_{R|d}(r)$ in (14) with $f_R(r)$ from Corollary 1 to get D2D coverage Γ_D^e. Similarly, we set $d = x$, $X = \{\rho_{max}, \rho_{mid}\}$ in (15) and take the expectation over X to obtain the cellular coverage Γ_M^e.
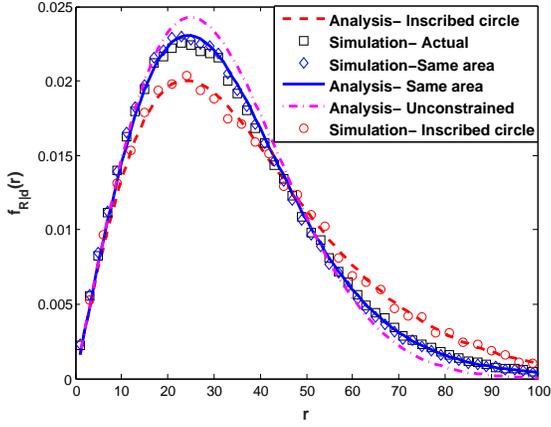
V. RESULTS AND PERFORMANCE EVALUATION

In this section, we will give some key results and verify our analysis with Monte Carlo simulations. For our simulation setup, the MBSs and D2D helpers are distributed according to HPPPs with intensities λ_M and λ_D respectively. For every iteration, the typical BS is placed at the origin before the cells are demarcated and the user is placed uniformly at a distance d from the typical BS[2]. The edge user is placed uniformly at a distance ρ_{mid} from the typical MBS at every iteration, where ρ_{mid} is the radius of the same area disk. The simulations are repeated 10,000 times. The values of the simulation parameters used in plotting the results are listed in Table I unless stated otherwise.
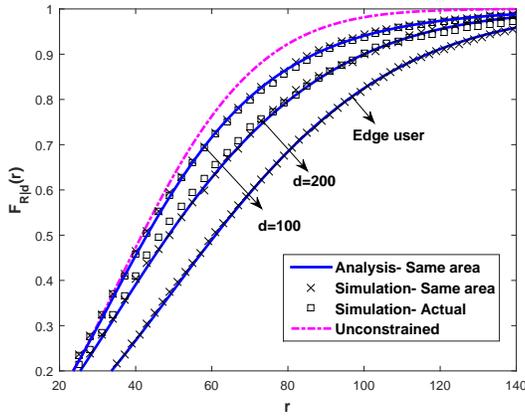
We first validate the distribution of distance derived in Theorem 1. Fig. 2a shows that the same area disk approximation is very accurate while the unconstrained nearest neighbor distribution as in [14] and the inscribed circle approximation deviate largely from the actual distribution of the distance between the tagged user and the nearest D2D helper within the cell. For a better comparison, we plot the CDF of the distance ($F_{R|d}(r) = \int_0^r f_{R|d}(y)dy$) in Fig. 2b. It is evident that the deviation of the distance distribution from the unconstrained nearest neighbor distribution is more pronounced as d increases and is maximum for the user at the cell edge.

Figs. 3 and 4 validate our analysis in Theorems 2 and 3. We can see from Fig. 4 that as d increases, Γ_M decreases. This is because the path loss for the link between the MBS

---

[2]The realizations in which the user lies outside the typical cell, or where no D2D helper is inside the cell, are all ignored.

(a) PDF.

(b) CDF. $\lambda_M = 10/\pi 500^2$

Figure 2: Distribution of distance to the nearest D2D helper from the tagged user within the Voronoi cell.

Figure 3: D2D coverage probability.

Figure 4: Cellular coverage probability.

and the tagged user increases. Even though the distance to the nearest interfering MBS also increases with the increase in d, as we make sure that the tagged user always remains inside the typical cell, the contribution of the path loss for the desired link is much higher. The D2D coverage Γ_D in Fig. 3 shows slight deviation from the simulations, which is because of the equi-dense HPPP approximation for the D2D interferers. As d increases, Γ_D also reduces. However, the effect of the increase in d is less pronounced on Γ_D compared to that on Γ_M. This is because in the cellular case, the increase in d translates into a rapid increase in path loss, but the distance to the nearest D2D helper for Γ_D does not scale in the same manner.

We now observe the behavior of the average cellular and D2D rates (R_M and R_D) with the variation in λ_M in Fig. 5. As expected, R_D is higher than R_M for a given set of parameters because of the short range D2D communication. For a fixed d, both R_M and R_D decrease with the increase in λ_M. This is because, the interference is aggravated as the cell size reduces with the increase in λ_M. The average cellular and D2D rates at the cell edge user (R_M^e and R_D^e) exhibit a
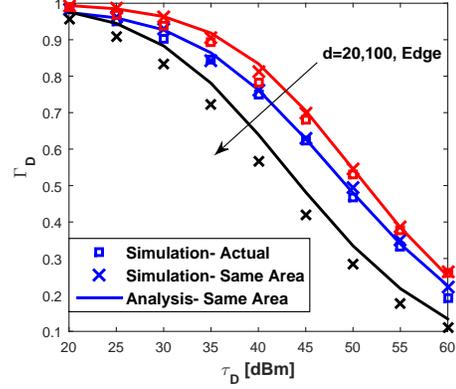
different behavior. We see that R_M^e does not vary with the increase in λ_M. This observation aligns with [14], where Γ_M shows the same behavior when the user is placed uniformly inside the cell. This is due to the fact that after averaging over the location of the tagged user in an interference limited scenario, Γ_M does not change with the change in the MBS density as the inverse relation of the path loss of the desired link and the interference perfectly cancels out. On the other hand, R_D^e initially decreases with the increase in λ_M and attains a minimum value and then begins to increase again. The increase is because the density of the interfering D2D helpers $\tilde{\lambda}_M$ does not scale linearly with λ_M as it depends on p_{act}, which decreases with the increase in λ_M.

We now wish to see the overall gain in the average LSE $T(i)$ compared to the LSE of the conventional cellular network without D2D, which is simply the cellular rate $T_{ref} = R_M$. Fig. 6 illustrates that for small values of d, the gains due to D2D communication can only be harnessed for ultra-dense cellular networks, but as d increases, D2D communication provides significant gains in the LSE. Fig. 7 displays how the cell edge user's LSE ($T^e(i)$) varies with content popularity parameters. Because R_M^e is constant, the changes in $T^e(i)$ are primarily governed by the changes in the D2D rate with respect to λ_M. As expected, high gains are achieved when a
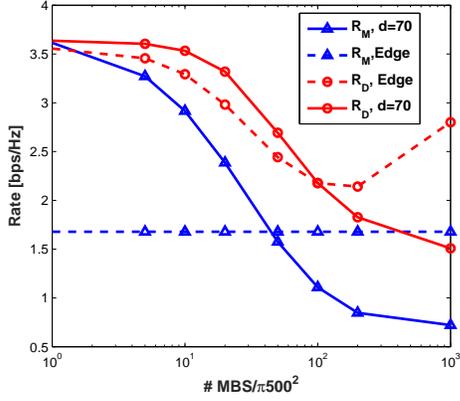
Figure 5: Cellular and D2D rates with respect to MBS density.

Figure 7: Variation in link spectral efficiency of the requesting user at the cell edge.
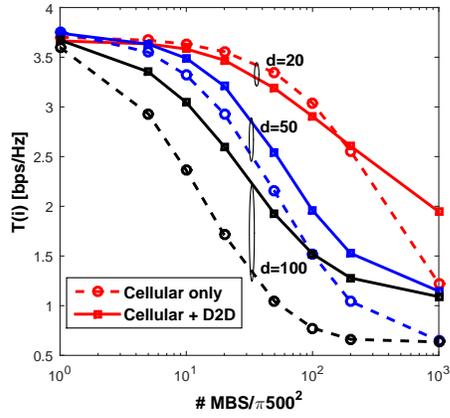

Figure 6: Variation in link spectral efficiency with respect to the MBS density for various values of d, $i = 1$.

popular content is requested and the popularity distribution is skewed, but λ_M has to be adapted to achieve maximum gains.

VI. CONCLUSION

In this paper, we presented a novel framework for the analysis of cellular networks with coordinated D2D communication. We derived the expressions for cellular and D2D coverage probabilities and the link spectral efficiency. We obtained the distribution of the distance between the tagged user and the nearest D2D helper within the cell using a same area disk approximation, which is shown to be fairly accurate. The results reveal that D2D communication is much more effective when the user is far from the BS and requests content with high popularity; and for the user placed at the cell edge, the MBS density has to be carefully tuned to achieve maximum performance gains.

APPENDIX A
PROOF OF THEOREM 1

The probability that the distance between the user and its nearest D2D helper within the cell is at least r is given as
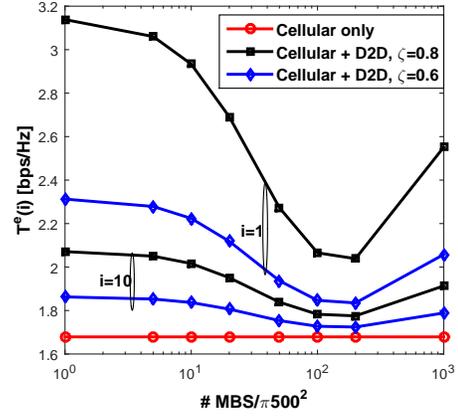
$$\mathbb{P}[R > r|X = x] = \exp(-\lambda_D A(r, d, x)), \qquad (16)$$

where $A(r, d, x)$ is the area of intersection between the disks $b(\mathbf{x}_t, r)$ and $b(\mathbf{o}, x)$. This area can be divided into two regimes given as follows.

Regime 1- When $b(\mathbf{x}_t, r)$ lies inside $b(\mathbf{o}, x)$, i.e. $0 < r < x - d$. The overlapping area in this case is straightforward and is given as $A_1(r) = \pi r^2$.

Regime 2- When $b(\mathbf{x}_t, r)$ partly overlaps $b(\mathbf{o}, x)$, i.e. $x - d < r < x + d$. The overlapping area in this case can be calculated as [20]

$$A_2(r, d, x) = r^2 \arccos\left(\frac{\kappa_1}{2dr}\right) + x^2 \arccos\left(\frac{\kappa_2}{2dx}\right) - \frac{1}{2}\sqrt{4d^2x^2 - \kappa_2^2}, \qquad (17)$$

where $\kappa_1 = r^2 + d^2 - x^2$ and $\kappa_2 = x^2 + d^2 - r^2$.

From (16), we get $\mathbb{P}[R \leq r|X = x] = 1 - \exp(-\lambda_D A(r, d, x))$. Differentiating with respect to r gives

$$f_{R|X=x}(r) = A'(r, d, x)\exp(-\lambda_D A(r, d, x)), \qquad (18)$$

where $A'(r, d, x)$ is the derivative of $A(r, d, x)$ with respect to r. Substituting (17) in (18) gives $f_{R|X=x}(r)$ in (9). To obtain the distribution of R in (9), we have to ensure the following conditions:

1) $X > d$, i.e. the tagged user lies within the typical cell. The truncated distribution of X is expressed as

$$f_{X|X>d}(x) = \frac{f_X(x)}{\int_d^\infty f_X(x)\,dx}, \ X = \{\rho_{max}, \rho_{mid}\}. \qquad (19)$$

2) There is at least one D2D helper inside the cell. The probability that at least one D2D helper is present inside the disk is given as

$$p_N = \int_d^\infty \mathbb{P}[N \geq 1|X = x]\,f_X(x)\,dx, \qquad (20)$$

where $\mathbb{P}[N \geq 1|X = x] = 1 - \exp\left(-\lambda_D \pi x^2\right)$.

Switching the limits for x in (9) and substituting (20), (17) and (9) into (8) gives the desired result.

APPENDIX B
PROOF OF THEOREM 2

Because only one D2D helper can be active at one channel in a given macrocell, we employ a key assumption that the active interfering D2D helpers constitute a HPPP[3] Θ_D with intensity $\tilde{\lambda}_M = p_{act} \times \lambda_M$. Here, $p_{act} = 1 - \left(1 + 3.5^{-1}\lambda_D/\lambda_M\right)^{-3.5}$ is the probability that at least one D2D helper is active in a cell. The interference is then expressed as $I_D = \sum_{\mathbf{z}_j \in \Theta_d} h_j \|\mathbf{z}_j\|^{-\alpha}$ and the Laplace transform of I_D is given as

$$
\begin{aligned}
\mathcal{L}_{I_D}\left(s_D\right) &= \mathbb{E}\left[\exp\left(-s_D \sum_{\mathbf{z}_j \in \Theta_d} h_j \|\mathbf{z}_j\|^{-\alpha}\right)\right] \\
&\stackrel{(a)}{=} \mathbb{E}_Q\left[\exp\left(-2\pi\tilde{\lambda}_M \int_q^\infty \frac{x}{1 + \frac{x^\alpha}{s_D}}\,dx\right)\right] \quad (21)
\end{aligned}
$$

where (a) follows from the generating functional of a HPPP and the exponential distribution of h. The lower limit of the integral in (21) represents the guard zone. Notice that the lower limit q in this case is governed by the nearest active D2D interferer, where $f_Q(q) = 2\pi\tilde{\lambda}_M q \exp(-\tilde{\lambda}_M \pi q^2)$ because of the equi-dense HPPP approximation. As $\tilde{\lambda}_M$ is quite small, we apply Jensen's inequality and take the expectation inside the exponential to achieve a tight bound in (14).

APPENDIX C
PROOF OF THEOREM 3

Since the distance of the tagged user to the MBS is fixed, (13) reduces to $\Gamma_M = \mathcal{L}_{I_M}\left(s_M\right)$. To characterize the Laplace transform of the interference from MBSs, we consider an arbitrary interfering MBS at a distance v from the typical MBS and y from the tagged user. The Laplace transform is then given as

$$
\begin{aligned}
\mathcal{L}_{I_M}\left(s_M\right) &= \mathbb{E}\left[\exp\left(-s_M \sum_{\mathbf{y}_j \in \Phi_M \setminus \mathbf{y}_0} h_j y^{-\alpha}\right)\right] \quad (22) \\
&= \exp\left(-2\pi\lambda_M \int_{\mathbb{R}^2}\left\{1 - \right.\right. \\
&\qquad\qquad \left.\left. \mathbb{E}_H\left[\exp\left(-s_M h y^{-\alpha}\right)\right]\right\} y\,dy\right), \quad (23)
\end{aligned}
$$

Using the cosine rule we get $y = \sqrt{v^2 + d^2 - 2\,d\,v\,\cos(\theta - \phi)}$. This gives

$$
\mathcal{L}_{I_M}\left(s_M\right) = \mathbb{E}_\phi\left[\exp\left(-\lambda_M \int_{\theta=0}^{2\pi} \int_{v_{min}}^\infty \frac{v}{1 + s^{-1}y^\alpha}dv\,d\theta\right)\right],
$$

where $v_{min} = 2d\cos(\theta - \phi)$ follows form the fact that the nearest interfering MBS is at least a distance $y = d$ apart from the tagged user. Employing Jensen's inequality by shifting the expectation operator inside the exponential, we obtain (15).

REFERENCES

[1] S. Woo, E. Jeong, S. Park, J. Lee, S. Ihm, and K. Park, "Comparison of Caching Strategies in Modern Cellular Backhaul Networks," in *Proceeding of the 11th annual international conference on Mobile systems, applications, and services.* ACM, 2013, pp. 319–332.

[2] X. Lin, J. Andrews, A. Ghosh, and R. Ratasuk, "An Overview of 3GPP Device-to-Device Proximity Services," *IEEE Communications Magazine*, vol. 52, no. 4, pp. 40–48, 2014.

[3] F. Malandrino, C. Casetti, and C.-F. Chiasserini, "Toward D2D-Enhanced Heterogeneous Networks," *IEEE Communications Magazine*, vol. 52, no. 11, pp. 94–100, 2014.

[4] A. Asadi, Q. Wang, and V. Mancuso, "A Survey on Device-to-Device Communication In Cellular Networks," *IEEE Communications Surveys & Tutorials*, vol. 16, no. 4, pp. 1801–1819, 2014.

[5] G. Fodor, E. Dahlman, G. Mildh, S. Parkvall, N. Reider, G. Miklós, and Z. Turányi, "Design Aspects of Network Assisted Device-to-Device Communications," *IEEE Communications Magazine*, vol. 50, no. 3, pp. 170–177, 2012.

[6] M. Haenggi, *Stochastic Geometry for Wireless Networks.* Cambridge University Press, 2012.

[7] X. Lin, J. G. Andrews, and A. Ghosh, "Spectrum Sharing for Device-to-Device Communication in Cellular Networks," *IEEE Transactions on Wireless Communications*, vol. 13, no. 12, pp. 6727–6740, 2014.

[8] H. ElSawy, E. Hossain, and M.-S. Alouini, "Analytical Modeling of Mode Selection and Power Control for Underlay d2d Communication in Cellular Networks," *IEEE Transactions on Communications*, vol. 62, no. 11, pp. 4147–4161, 2014.

[9] M. Afshang, H. S. Dhillon, and P. H. J. Chong, "Modeling and Performance Analysis of Clustered Device-to-Device Networks," *arXiv preprint arXiv:1508.02668*, 2015.

[10] A. Altieri, P. Piantanida, L. R. Vega, and C. G. Galarza, "On Fundamental Trade-offs of Device-to-Device Communications in Large Wireless Networks," *CoRR*, vol. abs/1405.2295, 2014. [Online]. Available: http://arxiv.org/abs/1405.2295

[11] D. Stoyan, W. S. Kendall, J. Mecke, and L. Ruschendorf, *Stochastic geometry and its applications.* Wiley New York, 1987, vol. 2.

[12] C. Fricker, P. Robert, J. Roberts, and N. Sbihi, "Impact of Traffic Mix on Caching Performance in a Content-Centric Network," in *IEEE Conference on Computer Communications Workshops (INFOCOM WKSHPS).* IEEE, 2012, pp. 310–315.

[13] S. A. R. Zaidi, M. Ghogho, and D. C. McLernon, "Information Centric Modeling for Two-tier Cache Enabled Cellular Networks," *IEEE International Conference on Communications (ICC)*, 2015.

[14] J. G. Andrews, F. Baccelli, and R. K. Ganti, "A Tractable Approach to Coverage and Rate in Cellular Networks," *IEEE Transactions on Communications*, vol. 59, no. 11, pp. 3122–3134, 2011.

[15] E. Bastug, M. Bennis, and M. Debbah, "Cache-Enabled Small Cell Networks: Modeling and Tradeoffs," in *11th International Symposium on Wireless Communications Systems (ISWCS).* IEEE, 2014, pp. 649–653.

[16] S. Foss and S. Zuyev, "On a Voronoi Aggregative Process Related to a Bivariate Poisson Process," *Advances in Applied Probability*, pp. 965–981, 1996.

[17] P. Calka, "The distributions of the smallest disks containing the poisson-voronoi typical cell and the crofton cell in the plane," *Advances in Applied Probability*, pp. 702–717, 2002.

[18] P. Calka and T. Schreiber, "Limit theorems for the typical poisson-voronoi cell and the crofton cell with a large inradius," *Annals of probability*, pp. 1625–1642, 2005.

[19] J.-S. Ferenca and Z. Nédaa, "On the size-distribution of poisson voronoi cells," *arXiv preprint cond-mat/0406116*.

[20] E. W. Weisstein, "Circle-circle intersection," 2003.

---

[3] The equi-dense HPPP assumptions ignores the correlations due to the position of helpers inside a cell, but is more tractable [8].